Information Geometry for Model Reduction of Dynamic Loads in Power Systems

Clifford C. Youn
Tufts University
Medford, MA, USA
clifford.youn@tufts.edu

Andrija T. Sarić
University of Novi Sad
Novi Sad, Serbia
asaric@uns.ac.rs

Mark K. Transtrum
Brigham Young University
Provo, UT, USA
mktranstrum@byu.edu

Aleksandar M. Stanković
Tufts University
Medford, MA, USA
astankov@ece.tufts.edu

***Abstract*—Load modeling has been extensively studied in power systems. The problem is intrinsically hard, as a simple description is sought for a large collection of heterogeneous physical devices. One aspect of model simplification has to do with the number of parameters needed to describe a dynamic load. With the rich tapestry of methods proposed in the literature as a backdrop, this paper introduces a new approach to simplify the load models and estimate the parameters. Our method is based on information geometry which combines information theory with computational differential geometry to derive global estimation results and shed a new light on difficulties commonly encountered when fitting widely used models to the measurement data. The results are compared with the literature using simulations on the IEEE 14 bus benchmark system.**

***Index Terms*—Information Geometry, Load Modeling, Power System Management, Power System Stability**

I. Introduction

Massive blackouts worldwide in the early 21st century brought attention to the importance of the quantitative understanding of power system dynamics [1]. Load characteristics have an important bearing on a system's stability. However, modeling the loads to find such characteristics is complicated because a typical load bus is composed of a myriad of diverse components. Furthermore, the load composition changes frequently, depending on many factors including weather conditions, time-scales (am *vs.* pm, weekdays *vs.* weekends, summer *vs.* winter, etc.) and economic conditions [2]. Therefore, load modeling and parameter identification is intrinsically a very challenging task.

Various loads connected to a power system can be modeled using simplified composite models. A widely used approach combines two different types of loads: a static load and a dynamic load. A static load model is expressed as algebraic functions of the bus voltage magnitude and frequency at a time and shows the relationship between power and voltage at that instant [3]. Lights and resistive loads are some examples of static loads. In addition, a static load model can be time-varying or stationary, possibly resulting in inaccuracies for short time modeling [4]. Dynamic load models have been introduced to better capture variations of load powers. Dynamics that are related to operation of motors fall into this class of load models. A dynamic load model is typically connected in parallel to a static load model to form a composite model (see [5] and references therein).

However, composite load models typically require tuning of a large number of parameters to properly model the system. Even extensive field measurement data are often perceived as insufficiently rich to allow for well-behaved estimation of numerous parameters. Therefore, many papers (nicely reviewed in [5]) focused on reducing the number of parameters. Studies suggested that the parameter space is very anisotropic in the sense that variations in some directions in the parameter space may have orders of magnitude more effect on the system response than some other (possibly spatially close) directions. The effect of elimination of superfluous or less important parameters on the estimation procedure is often drastic, while maintaining the response very similar to the one obtained from the original (unreduced) composite load model.

One broad class of methods for detecting unimportant parameters is based on sensitivity considerations. The influential paper [5] calculated the sensitivity along the evolving system trajectory by utilizing the Jacobian matrix of measurement data. Another approach presented in [6] used the sensitivity information derived from the eigenvalues of the Hessian matrix. Both methods follow the determination of unimportant parameters with a separate procedure to tune the remaining (important) parameters. Later in this paper, an alternative approach based on information geometry will be introduced, which combines information theory with computational differential geometry. Our approach identifies unimportant parameters one by one, and re-tunes the remaining parameters at each stage.

The remainder of the paper is organized as follows: Section II is a brief description of the composite load model structure and its parameters; Section III discusses the parameter reduction using local or sensitivity methods, followed by the information geometry or global approach described in Section IV; Section V presents simulation results for the two classes of methods using example from [5], while brief conclusions and topics for the full paper are outlined in Section VI.

II. Composite Load Model

To effectively represent the complex power system component, a composite load model, which is a combination of static and dynamic parts, will be used in this paper. Constant (real and reactive) impedance (Z), constant (real and reactive) current (I) and constant (real and reactive) power (P) – also known as ZIP load – form the static load model. An induction

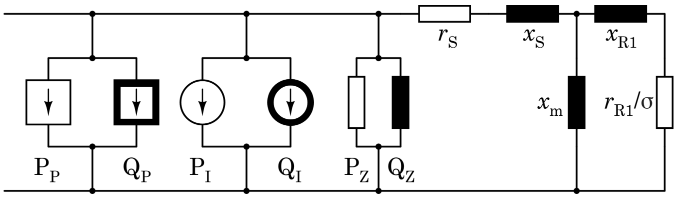

Fig. 1: Equivalent circuit for composite load model.

machine (IM) is used to capture the dynamic portion. The overall equivalent circuit for this composite load model is presented in Fig. 1.

A. Static Load Model

The static, or ZIP, load is shown in the left part of Fig. 1 and can be described as in [7]:

$$\begin{aligned} p_h &= -\left[p_z\left(\frac{v_h}{v_0}\right)^2 + p_i\left(\frac{v_h}{v_o}\right) + p_p\right] \\ q_h &= -\left[q_z\left(\frac{v_h}{v_0}\right)^2 + q_i\left(\frac{v_h}{v_o}\right) + q_p\right] \end{aligned} \tag{1}$$

where p_h and q_h are active and reactive powers, respectively. p_z, p_i, p_p and q_z, q_i, q_p represent the coefficients for ZIP load parameters. v_h refers to bus voltage magnitude and v_0 is the initial voltage at the load bus.

B. Dynamic Load Model

The dynamic portion of the load, or induction machine, is pictured in the right part of the Fig. 1, where r_S and x_S are the resistance and reactance of the stator, respectively; r_{R1} and x_{R1} are the resistance and reactance of the rotor, respectively; x_m is magnetizing reactance; σ is the slip in p.u., satisfying $\sigma = 1-\omega$, while ω is the speed of the machine. e'_d and e'_q refer to $d-$ and $q-$ axis transient EMF. The equivalent induction machine can be written as [7]:

$$\begin{aligned} \dot{\sigma} &= \frac{1}{2H_m}[(\alpha + \beta\sigma + \gamma\sigma^2) - (e'_d i_d + e'_q i_q)] \\ \dot{e'_d} &= \Omega_b \sigma e'_q - \frac{1}{T'_0}[e'_d + (x_0 - x')i_q] \\ \dot{e'_q} &= -\Omega_b \sigma e'_d - \frac{1}{T'_0}[e'_q - (x_0 - x')i_d] \end{aligned} \tag{2}$$

where

$$\begin{aligned} x_0 &= x_S + x_m \\ x' &= x_S + \frac{x_{R1}x_m}{x_{R1} + x_m} \\ T'_0 &= \frac{x_{R1} + x_m}{\Omega_b r_{R1}} \end{aligned} \tag{3}$$

α, β and γ are the coefficients for the mechanical torque, which satisfy $\alpha + \beta + \gamma = 1$; H_m is the machine rotor inertia constant; Ω_b is the base synchronous frequency in rad/s. Finally, active and reactive powers of the induction machine can be derived using following equations:

$$\begin{aligned} v_d - e'_d &= r_S i_d - x' i_q \\ v_q - e'_q &= r_S i_q + x' i_d \end{aligned} \tag{4}$$

$$\begin{aligned} p_h &= -(v_d i_d + v_q i_q) \\ q_h &= -(v_q i_d - v_d i_q) \end{aligned} \tag{5}$$

where $v_d = -v_h \sin\theta$ and $v_q = v_h \cos\theta$ represent $d-$ and $q-$ axis bus voltages; i_d and i_q refer to $d-$ and $q-$ axis stator currents.

From (1)-(3), the total number of parameters that need to be identified is eleven: $p_z, p_i, p_p, q_z, q_i, q_p$ from the ZIP load and $r_S, x_S, r_{R1}, x_{R1}, x_m$ from the induction machine.

III. Parameter Reduction - Local Sensitivity

Load characteristics are generally written in the differential-algebraic equation (DAE) form as:

$$\begin{aligned} \dot{x} &= f(x, z, p, t) \\ 0 &= g(x, z, p, t) \end{aligned} \tag{6}$$

where x are state variables, z are the algebraic variables, p are parameters, and t is the time variable. Next, parameters are to be estimated from the measurements (y) below:

$$y = h(x, z, p, t) \tag{7}$$

Sensitivity is then found by calculating the Jacobian matrix $\mathbf{J} = \partial h(t)/\partial p$, which is the first partial derivatives of measurement vector with respect to each parameter.

Reference [8] presented one of the first complete local analyses that utilized the sensitivity to select the parameters for model reduction. The so called *subset selection* for parameter estimation is achieved by partitioning the parameters into *well-conditioned* parameters and *ill-conditioned* parameters prior to estimation. The exclusion of ill-conditioned parameters (fixed to priors) from the estimation makes the procedure much better conditioned (at a price of a possible bias).

To sort the parameters into well- and ill-conditioned, the Hessian matrix ($\mathbf{H}$)[1] should be computed first. For small residuals or increments, Hessian can be expressed as $\mathbf{H}(\theta) \approx \mathbf{J}'(\theta)\mathbf{J}(\theta)$ where θ is the parameter vector. This Hessian matrix ($\mathbf{H}$) is (i) symmetric and positive semidefinite (eigenvalues thus being real and non-negative); and (ii) usually nearly singular, implying that the matrix has very large condition number $\kappa(\mathbf{H})$.

To separate the parameters, eigenvalues are found using eigendecomposition of $\mathbf{H}$ by $\mathbf{H} = \mathbf{V}\Lambda\mathbf{V}'$. Then, the matrix $\mathbf{V}$ is partitioned into $\mathbf{V} = [\mathbf{V}_\rho\ \mathbf{V}_{n-\rho}]$ where $\mathbf{V}_\rho$ includes the first ρ columns of $\mathbf{V}$. Here, ρ is the number of eigenvalues that are much larger than the remaining $n-\rho$ ones. Then, QR decomposition is performed to find the permutation matrix ($\mathbf{P}$).

$$\mathbf{V}'_\rho \mathbf{P} = \mathbf{QR} \tag{8}$$

The permutation matrix ($\mathbf{P}$) is used to reorder the parameters so that the parameters can be divided into the well-conditioned (first ρ) and ill-conditioned (last $n-\rho$) parameters. Finally, additional processes such as nonlinear least squares parameter estimation approach are required to estimate the ρ "good" parameters [9].

[1]Either the Jacobian or Hessian matrix can be used but [8] adopted the Hessian since eigenvalues and eigenvectors are more familiar than the singular values and singular vectors

IV. Global Sensitivity via Information Geometry

The premise of our approach is that a model with many parameters is a mapping from a parameter space into a data or prediction space. Recent study [10] suggested that the model with multiple parameters are usually *sloppy*, which is a term to explain a complex model exhibiting large parameter uncertainty when fit to data. A key difficulty in dealing with models of complex systems is the highly anisotropic mapping between the parameters and data spaces, meaning that small variations in parameter space may lead to dramatic changes in the measurement (data) space while other variations in parameters can lead to no discernible change in the model behavior.

The information geometry approach explores the anisotropies in the parameter space by focusing on a data (measurement) space and by quantifying the model manifold (corresponding to predictions for all allowed parameter variations) in that space [10]. It turns out that the manifold is typically bounded, with a hierarchy of widths that generalizes the hierarchy of eigenvalues of the Hessian matrix ($\mathbf{H}$). The approach has a number of useful properties for nonlinearly parametrized models including [11]: (i) the model manifold retains all the information – it is equivalent to the original model mathematically; (ii) the model, which is the manifold embedded in data space, is separated from the particular data point being fit; (iii) since the parameters will work as local coordinates on the manifold, no matter how the model is re-parameterized, the set of points on the model manifold remains the same; (iv) the Riemannian distance metric on the model manifold is the Fisher Information Matrix (FIM). Information geometry therefore serves as a natural bridge between the local analysis and the global analysis.

A key tool for studying the model manifold are geodesic curves – analog of straight lines on curved surfaces. They are calculated numerically as the solution to a second order ordinary differential equation in parameter space that involves first and second order sensitivities [12]. Derivation of these expressions by hand can be tedious and error prone (particularly for large models). Automatic differentiation was used to simplify the process.

Our model reduction procedure applies the manifold boundary approximation method (MBAM) procedure from [13]. Parametric degrees of freedom are systematically removed, one at a time, by approximating the full manifold by its boundary. For n parameters, the manifold will be an n-dimensional surface. The key point in this MBAM is that the boundaries of an n-dimensional manifold are themselves actually $(n-1)$-dimensional manifolds. The boundaries represent a model with one parameter less. After several approximation steps, the reduced model is represented by a hyper-corner of the original manifold that, if successful, preserves most of the original model's behavior.

Reaching the boundaries from an initial point in the shortest path on the curved manifold implies motion along a *geodesic* which is a solution to the following second-order differential equations:

$$\frac{d^2x^k}{ds^2} + \Gamma^k_{ij}\frac{dx_i}{ds} \cdot \frac{dx_j}{ds} = 0 \tag{9}$$

where Γ^k_{ij} is the Christoffel symbol that contains curvature information about the mapping between the parameter space and data space. Whether the geodesic has reached the boundaries or not can be determined by the parameter velocities, a rate of change of the parameters with respect to s, the geodesic "time." When the geodesic reaches the boundary, then the parameter velocities either increase or decrease significantly, as shown in Fig. 2.

V. Simulation Results

The standard simulation environment was built on IEEE 14-bus test system (Fig. 3) in Matlab. PSAT, a Matlab toolbox for power system analysis and simulation, was used to calculate the system's sensitivities and outputs. Details of the PSAT can be found in [14]. Julia was used for differential geometry computation.

A. Local Sensitivity

The parameters are shown in the vector below:

$$\theta = [r_S \;\; x_S \;\; r_{R1} \;\; x_{R1} \;\; x_m \;\; p_z \;\; p_i \;\; p_p \;\; q_z \;\; q_i \;\; q_p]' \tag{10}$$

In order to find the eigenvalues and permutation matrix ($\mathbf{P}$), eigendecomposition is applied to the Hessian matrix ($\mathbf{H}$). Resulting eigenvalues are presented below:

$$\begin{matrix} 8.39e^{-15} & 2.42e^{-13} & 3.65e^{-13} & 8.53e^{-13} & 1.35e^{-11} \\ 1.63e^{-7} & 8.59e^{-6} & 1.01e^{-2} & 7.12e^{-1} & 3.22 \;\; 8.20e^{3} \end{matrix} \tag{11}$$

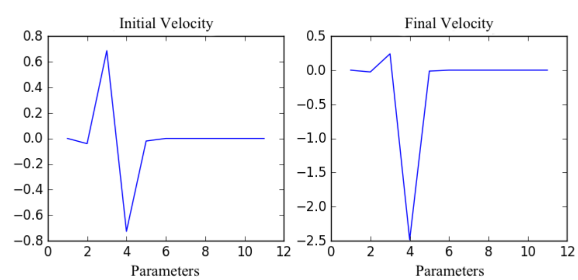

(a) After first iteration: fourth parameter (x_{R1}) reaches limit in *negative* region

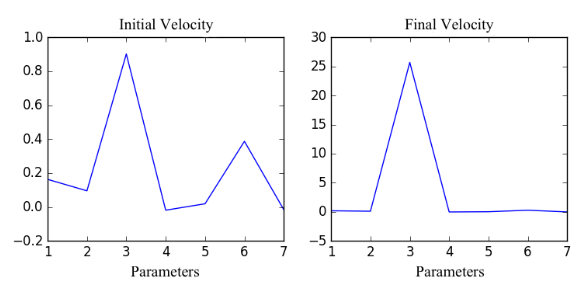

(b) After fifth iteration: third parameter (x_m) reaches limit in *positive* region

Fig. 2: Initial and final velocity for each component

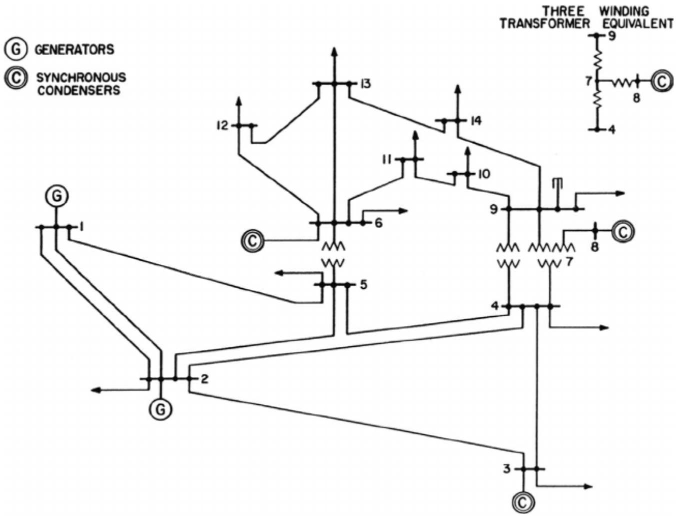

Fig. 3: IEEE 14-bus system - Static and dynamic loads are connected to bus #14

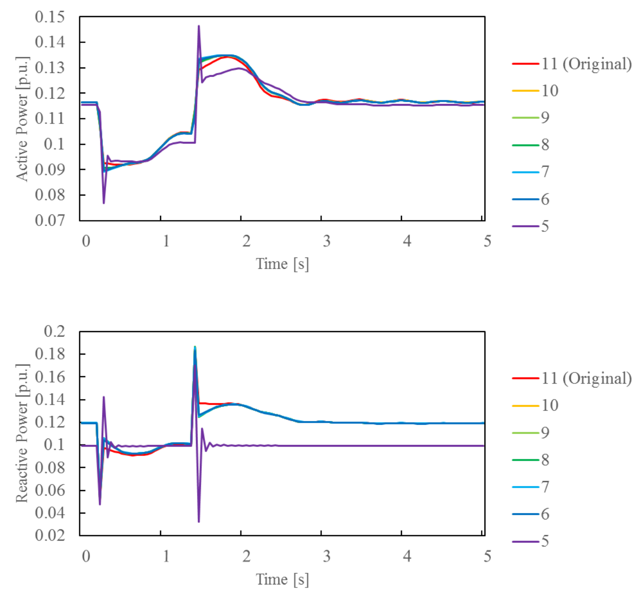

Fig. 4: Outputs for composite load model (including both static and dynamic load model) after parameter reductions with fault at bus #5. Numbers indicate the remaining parameters.

This matrix is extremely ill-conditioned, since the condition number $\kappa(\mathbf{H})$ is $9.78e^{17}$. The first five eigenvalues $(n-\rho)$ are relatively smaller than the remaining six eigenvalues (ρ), implying that five parameters can be fixed and remaining six parameters are to be estimated. To match the parameters with eigenvalues for partitioning, parameter vector θ is rearranged using the permutation matrix ($\mathbf{P}$) by applying to $\tilde{\theta} = \mathbf{P}'\theta$.

$$\tilde{\theta} = [x_S \;\; r_S \;\; p_i \;\; p_p \;\; q_z \;\; r_{R1} \;\mid\; p_z \;\; x_{R1} \;\; x_m \;\; q_i \;\; q_p]' \tag{12}$$

In the rearranged parameter vector $\tilde{\theta}$, the following five parameters, $p_z, x_{R1}, x_m, q_i, q_p$ at the end of the vector are to be fixed to priors. A separate computation is required to estimate the well-behaved parameters.

B. Global Sensitivity via Information Geometry

The procedure starts by finding the initial direction of the parameter variation and solving for the geodesic using the FIM. Eigenvectors of the FIM point out directions and eigenvalues are utilized to determine the velocity (rate of change, in log coordinates) of each parameter.

After the first iteration, the velocity components for each parameter are shown in Fig. 2a. From this, it can be concluded that the fourth parameter, x_{R1}, has reached the limit in the *negative* (log) region, thus becoming zero. On the other hand, if the final velocity of the components reaches the limit in the *positive* region like in Fig. 2b, then it means that the corresponding parameter tends to infinity, resulting in *open circuit*.

The simulations were performed for two different situations with faults occurring at bus #4 and bus #5 in Fig. 3. Both simulations have shown that the suggested information geometry approach was able to reduce five parameters – r_S, x_{R1}, x_m, p_i, q_i, while largely tracking the original eleven-parameter model output as in Fig. 4. Removing one more additional parameter showed visible difference in the output, that can be captured, for example, by mean squared errors are shown in Table I and the new parameters for the reduced model are shown in Table II.

It is instructional to interpret our results in terms of the equivalent circuit in Fig. 1 using (1). Since both p_i and q_i are reduced, remaining components from ZIP load are expected to have larger influence as a result, which is indeed the case. Also with x_m open, it is reasonable to think of equivalent impedances in the remaining branch, thus leaving one resistance (r_{R1}) and one reactance (x_S).

When the results from local analysis are compared with the results from global analysis, they are consistent in the terms of numbers of parameters to be reduced (five in both), and largely in parameters to be reduced (three out of five are the same - x_{R1}, x_m, q_i). Interestingly, five out of six of our "good" parameters are also contained in the somewhat more optimistic list of eight "good" parameters in [5]. We are also encouraged by the robustness of our procedure in terms of fault locations used to initiate the transients.

C. Sub-models

Simulation results presented in this paper were so far based on composite load models, which includes both static and dynamic load models. Now, the simulations for each load sub-model were tried to see how the information geometry approach will work on each case. In case of dynamic load model (induction machine), the results showed that this method could reduce two parameters (x_{R1} and r_S) from five parameters while still maintaining the original characteristics (Fig. 5). Meanwhile, for static load model (ZIP load), also two parameters (p_i and q_i) can be reduced from original six

TABLE I: Mean square error (MSE) for reduced parameter model, $\times e^{-4}$

			Number of remaining parameters					
			10	9	8	7	6	5
Fault at Bus #4	P_h (Active Power)	0-10 sec (with transient)	45	45	47	59	55	1054
		0-5 sec (without transient)	89	89	93	118	110	1461
	Q_h (Reactive Power)	0-10 sec (with transient)	114	114	115	111	129	342
		0-5 sec (without transient)	227	226	228	231	236	611
Fault at Bus #5	P_h (Active Power)	0-10 sec (with transient)	38	36	39	52	47	172
		0-5 sec (without transient)	75	72	77	103	94	332
	Q_h (Reactive Power)	0-10 sec (with transient)	109	109	109	106	96	1485
		0-5 sec (without transient)	217	217	218	211	192	2274

TABLE II: Estimated parameters after information geometry approach

Parameters		p_z	p_i	p_p	q_z	q_i	q_p	r_S	x_S	r_{R1}	x_{R1}	x_m
Initial condition (eleven parameters)		0.333	0.333	0.333	0.333	0.333	0.333	0.010	0.150	0.050	0.150	5.000
After simulation (six parameters)	Fault at Bus #4	0.489	≈ 0	0.502	0.658	≈ 0	0.514	≈ 0	0.325	0.077	≈ 0	$\approx \infty$
	Fault at Bus #5	0.485	≈ 0	0.506	0.667	≈ 0	0.515	≈ 0	0.328	0.076	≈ 0	$\approx \infty$

parameters (Fig. 6). Reduced parameters were all part of the five parameters that were derived for composite load models. Notice that if the IM sub-model analysis were performed separately, x_m still remains. This can be interpreted from a circuit point of view – in the case of the full composite model, even after reducing the x_m, remaining parameters (p_z, p_p, q_z, q_i) could match the response (Fig. 1). However, in the IM dynamic load only sub-model, there is no other reactance shunt component that can perform that role.

Also, in the Fig. 5 and 6, the dynamic loads have sharper fluctuations, which are largely absent for the static loads sub-model. These features indirectly support the practice of combining static and dynamic sub-models to describe the actual loads.

D. Mismatches Among Model Classes

This is an important practical issue, as there is often considerable uncertainty about the nature of the load. The effects of model mismatches have been explored through simulation. It is clear from the preceding analysis that simply adopting the most detailed model is not a wise strategy given the concomitant parameter uncertainty.

Simulation results are presented in Table III, where ◯ represents the parameters that are suggested for reduction and $\times$ shows the parameters whose additional removal leads to unacceptable match between the (reduced) model response and the recorded transient, thus stopping the overall model reduction procedure. Case #5 is the matching classes model (the most detailed model) that was discussed in previous subsection V-B for comparison.

It is clear that our conclusions about model structure are remarkably robust, as the list of "well behaved" parameters remains largely unchanged (Table III) and the outputs from the "reduced class" model show strong similarities to the "most detailed" model (composite load model) as shown in Fig. 7.

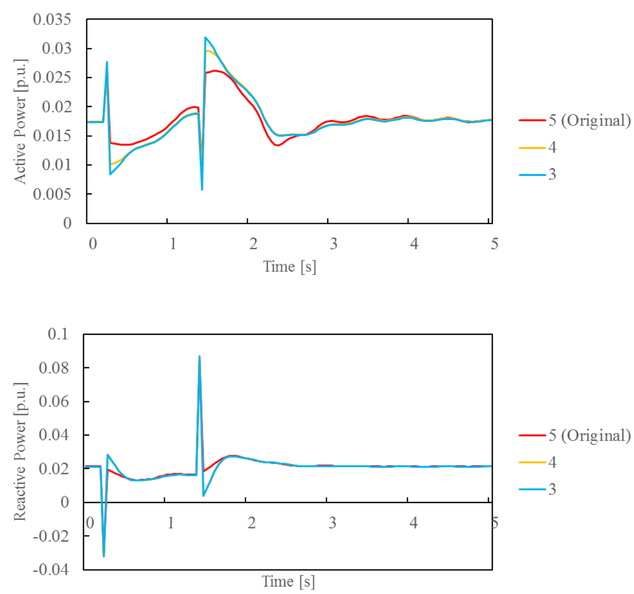

Fig. 5: Outputs for dynamic load sub-model (induction machine) after parameter reduction, with fault at bus #5. Numbers indicate the remaining parameters.

VI. Conclusion

This paper introduces a new approach for load model reduction that is based on information geometry. It produces useful practical results that complement and extend the local analysis for composite load models. Data collected online and real-time can be used to examine the situation more quickly by using the reduced load model. The procedure is applicable to other forms of load models (e.g., exponential recovery) and benefits from wider availability of wide-bandwidth recording devices such as Phasor Measurement Units (PMUs). The influence

TABLE III: Parameters eligible for reduction among mismatching model classes

Case	True Model	Assumed	p_z	p_i	p_p	q_z	q_i	q_p	r_S	x_S	r_{R1}	x_{R1}	x_m
#1	ZIP & IM	ZIP	×	○			○	○					
#2	ZIP & IM	IM								○	×	○	
#3	ZIP	ZIP & IM		○		×	○		○			○	○
#4	IM	ZIP & IM		○			○	×	○			○	○
#5	ZIP & IM	ZIP & IM		○			○		○		×	○	○

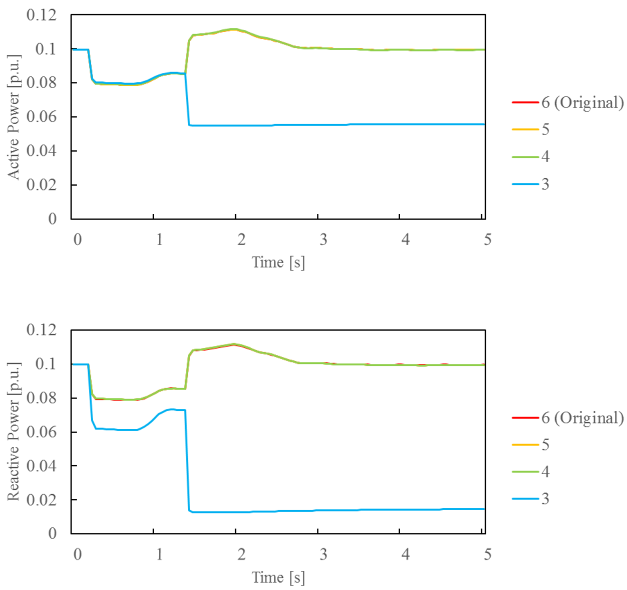

Fig. 6: Outputs for static load sub-model (ZIP load) after parameter reductions with fault at bus #5. Numbers indicate the remaining parameters.

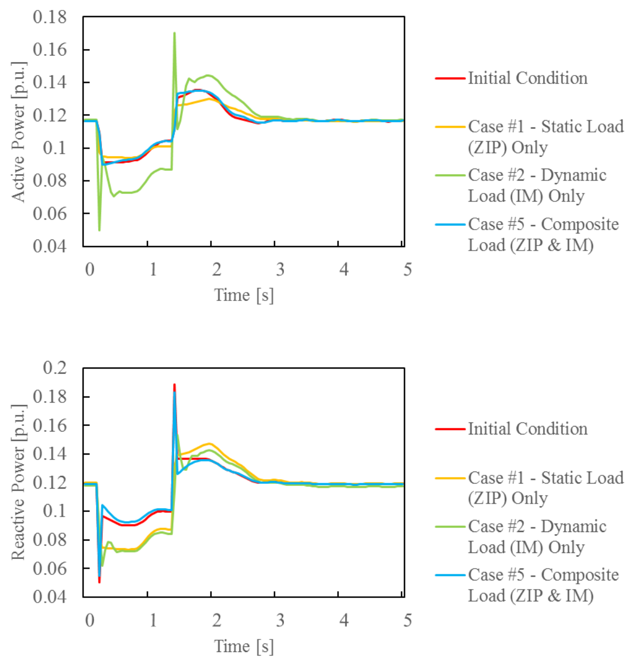

Fig. 7: Outputs based on parameter reductions for case #1, #2 and #5 of Table III with fault at bus #5.

of the types of transient recordings available remains to be quantified, and we hope that the global parameter identification procedure will remain effective and robust.

REFERENCES

[1] G. Andersson, P. Donalek, R. Farmer, N. Hatziargyriou, I. Kamwa *et al.*, "Causes of the 2003 major grid blackouts in north america and europe, and recommended means to improve system dynamic performance," *IEEE transactions on Power Systems*, vol. 20, no. 4, pp. 1922–1928, 2005.

[2] P. Kundur, N. J. Balu, and M. G. Lauby, *Power system stability and control*, vol. 7, ch. 7, pp. 271–314.

[3] J. A. Momoh, *Electric power system applications of optimization*. CRC Press, 2008, ch. 2, pp. 17–62.

[4] W.-S. Kao, C.-T. Huang, and C.-Y. Chiou, "Dynamic load modeling in taipower system stability studies," *IEEE Trans. on Power Systems*, vol. 10, no. 2, pp. 907–914, 1995.

[5] J. Ma, D. Han, R.-M. He, Z.-Y. Dong, and D. J. Hill, "Reducing identified parameters of measurement-based composite load model," *IEEE Trans. on Power Systems*, vol. 23, no. 1, pp. 76–83, 2008.

[6] S. Son, S. H. Lee, D.-H. Choi, K.-B. Song, J.-D. Park *et al.*, "Improvement of composite load modeling based on parameter sensitivity and dependency analyses," *IEEE Trans. on Power Systems*, vol. 29, no. 1, pp. 242–250, 2014.

[7] F. Milano, *Power system modelling and scripting*. Springer Science & Business Media, 2010, ch. 14, pp. 313–324. [Online]. Available: http://dx.doi.org/10.1007/978-3-642-13669-6

[8] M. Burth, G. C. Verghese, and M. Vélez-Reyes, "Subset selection for improved parameter estimation in on-line identification of a synchronous generator," *IEEE Trans. on Power Systems*, vol. 14, no. 1, pp. 218–225, 1999.

[9] C.-T. Huang, Y.-T. Chen, C.-L. Chang, C.-Y. Huang, H.-D. Chiang, and J.-C. Wang, "On-line measurement-based model parameter estimation for synchronous generators: model development and identification schemes," *IEEE Trans. on Energy Conversion*, vol. 9, no. 2, pp. 330–336, 1994.

[10] M. K. Transtrum, B. B. Machta, K. S. Brown, B. C. Daniels, C. R. Myers, and J. P. Sethna, "Perspective: Sloppiness and emergent theories in physics, biology, and beyond," *The Journal of Chemical Physics*, vol. 143, no. 1, p. 010901, 2015.

[11] B. K. Mannakee, A. P. Ragsdale, M. K. Transtrum, and R. N. Gutenkunst, *Sloppiness and the Geometry of Parameter Space*. Springer International Publishing, 2016, pp. 271–299. [Online]. Available: http://dx.doi.org/10.1007/978-3-319-21296-8_11

[12] M. K. Transtrum, A. T. Saric, and A. Stankovic, "Measurement-directed reduction of dynamic models in power systems," *IEEE Trans. on Power Systems*, 2016, (in press).

[13] M. K. Transtrum and P. Qiu, "Model reduction by manifold boundaries," *Physical Review Letters*, vol. 113, no. 9, p. 098701, 2014.

[14] F. Milano. Power system analysis toolbox (PSAT). [Online]. Available: http://faraday1.ucd.ie/psat.html